SPIE's NDE and Smart Structures Symp., Paper 4702-40, San Diego, CA, March 2002

Interaction of high intensity focused ultrasound with biological materials

Ajit Mal*, Feng Feng, Michael Kabo, Jeffrey Wang
University of California, Los Angeles, CA 90095

Yoseph Bar-Cohen
Jet Propulsion Laboratory, Pasadena, CA 91109

ABSTRACT

This work is motivated by possible medical applications of focused ultrasound in minimally invasive treatment of a variety of disorders. The mechanical and thermal effects caused by high-frequency ultrasound in different material systems are calculated using a finite element based program called PZflex. The pressure distributions generated by plane as well as focused ultrasound beams are presented. For the focused beam, the temperature distribution in the focal zone is also calculated. The results indicate that the heating efficiency of the ultrasound energy in the focal region depends on the exciting frequency and the geometry of the focal zone depends on the material being tested. At higher excitation energies, cavitation and nonlinear effects need to be included in the simulations. These effects are under current investigation.

Keywords: Focused ultrasound, HIFU, PZFlex, Finite Element Method (FEM), Thermal Field.

1. INTRODUCTION

The interaction between ultrasound and biological matters has been investigated by a number of authors for almost half a century[1-8]. However, the widespread use of therapeutic ultrasound in clinical environments has so far been limited, in part, due to incomplete understanding of the interaction process. In order to treat a narrow target area with minimal damage to the surrounding tissue, it is necessary to predict the path of the ultrasound beam from the transducer to the target. Since experimental studies using living tissue is difficult and costly, theoretical simulation of the problem can be extremely useful in providing a firm scientific basis for future clinical applications of focused ultrasound. Furthermore, the complex geometry and acoustic properties of human tissue often preclude their treatment using analytical methods and numerical methods (e.g., finite element or FEM) are needed in order to obtain quantitative information on the interaction between ultrasound and biological materials.

In this study, PZFlex[5], a commercially available finite element based software, is used to obtain numerical solution of a variety of models of the interaction problem. PZFlex is widely used for designing transducers [6], calculating the mechanical effects of the ultrasound on tissues [7], modeling therapeutic ultrasound [8] and calculating thermal effects of high-frequency ultrasound [9]. For this reason, PZFlex has recently emerged as a very useful tool in analyzing the mechanical, thermal, biological and clinical aspects of therapeutic ultrasound.

In this paper, the mechanical and thermal effects caused by high-frequency ultrasound in different material systems are calculated. The pressure and temperature distributions generated by a focused ultrasound in the material systems are calculated and presented. Finally, the direction of future research is discussed.

2. PLANE WAVES

In most applications of ultrasound, the objective is to treat a small area in the path of the ultrasonic beam. Thus, the theoretical simulations must be able to isolate the local effects associated with the interaction process from boundary and other effects. However, conventional Finite Element Methods

* Correspondence: ajit@ucla.edu, Tel: (310)-825-5481, Fax: (301)-206-4830, http://www.seas.ucla.edu/~ajit

require the models to have finite dimensions with specified conditions at the boundary. In dealing with wave local interaction effects with small geometric and material features in extended media, many modern FEM packages use boundary conditions that approximately simulate the radiated energy out of the FEM model. Two such conditions, namely, symmetry (SYMM) and absorption (ABSR) are used in simulating propagation in unbounded media. In order to verify the accuracy of these approximations, the problem of plane waves propagating across a solid layer between two different fluid media is considered. The analytical solution of this problem is compared with that obtained from PZflex in an effort to insure the accuracy of the FEM code for unbounded media.

2.1 Problem description

The three-layered materials system is shown in Fig. 1. It is infinite in the vertical, y-direction and semi-infinite along the positive x direction. The thickness of the water layer is h_1 and that of the solid layer is h_2. A uniformly distributed pressure, f*(t)*, is applied at $y = 0$.

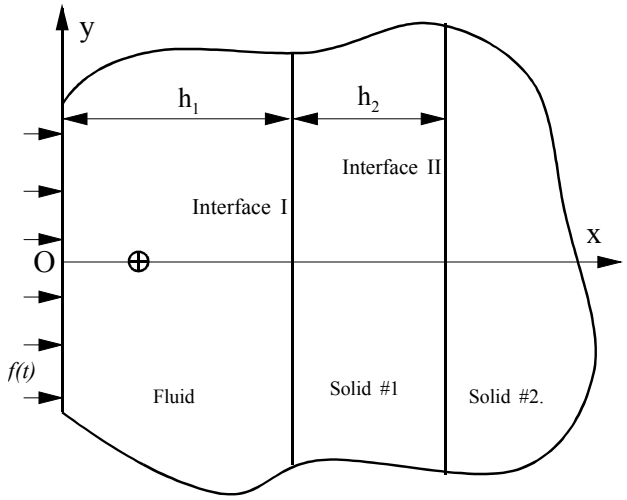

Fig. 1: A three-layered medium

2.2. Theoretical solution

The pressure field within the medium can be calculated by using a standard theoretical approach. We first solve the propagation problem in the frequency domain and invert the resulting spectral response to obtain the time domain result. In the frequency domain, the displacement in water can be expressed in the form

$$W_1(x,\omega) = C\left[e^{-ik_1(x-h_1)} + R\cdot e^{ik_1(x-h_1)}\right],\ 0 < x < h_1 \tag{1}$$

where the time dependence, $e^{i\omega t}$, has been suppressed. In (1), $k_1 = \omega/\alpha$, is the wave number, ω is the angular frequency, α_1 is the velocity of the acoustic waves in water and R is the reflection coefficient. The displacements in the 2nd and 3rd layers are of the form

$$W_2(x,\omega) = Ae^{-ik_2(x-h_1)} + Be^{ik_2(x-h_1)},\ 0 < x < h_1 \tag{2}$$

$$W_3(x,\omega) = Te^{-ik_3(x-h)},\ h_1 < x < h \tag{3}$$

where $h = h_1 + h_2$, $A, B,$ are constants, T is the transmission coefficient, and k_1, k_2 are the wavenumbers in the *2nd* and *3rd* layers, related to the wave velocities, α_1, α_2, through $k_j = \omega/\alpha_j$.

The pressure is related to the displacement through the relation

$$P(x,\omega) = (\lambda + 2\mu)\frac{\partial w}{\partial x} = \rho\alpha^2\frac{\partial w}{\partial x} \tag{4}$$

Applying the conditions for the pressure at x = 0 and the continuity conditions for the pressure and displacement at the interfaces, $x = h_1, h$, the following system of equations is obtained for the unknown coefficients, C, R, A, B, and T:

$$\begin{cases} i\omega Z_1 C e^{ik_1 h_1} = F(\omega) \\ \dfrac{F(\omega)}{i\omega Z_1}(1+R)e^{-ik_1 h_1} = A + B \\ F(\omega)(-1+R)e^{-ik_1 h_1} = i\omega Z_2(-A+B) \\ Ae^{-ik_2 h_2} + Be^{ik_2 h_2} = T \\ -Ae^{-ik_2 h_2} + Be^{ik_2 h_2} = -Z_{32}T \end{cases} \tag{5}$$

where

$$Z_i = \rho_i \alpha_i,\ Z_{ij} = \frac{\rho_i \alpha_i}{\rho_j \alpha_j}$$

and $F(\omega)$ is the Fourier time transform of the applies pressure, $f(t)$. In the present calculations $f(t)$ is assumed to be a single cycle sine pulse of period τ given by

$$f(t) = \sin(\frac{2\pi t}{\tau})H(t-\tau) \tag{6}$$

Thus

$$F(\omega) = \int_0^\infty f(t)e^{-i\omega t}dt = 2\frac{\pi\tau(e^{-i\tau\omega}-1)}{\omega^2\tau^2 - 4\pi^2} \tag{7}$$

Solving the system of equations, we obtain,

$$C = \frac{F(\omega)e^{-ik_1 h_1}}{i\omega Z_1}$$

$$R = -\frac{(k_2\alpha_2 Z_3 - k_1\alpha_1 Z_1)(e^{i2k_2h_2}+1) - (k_1\alpha_1 Z_1 Z_{32} - k_2\alpha_2 Z_2)(e^{i2k_2h_2}-1)}{(k_2\alpha_2 Z_3 + k_1\alpha_1 Z_1)(e^{i2k_2h_2}+1) + (k_1\alpha_1 Z_1 Z_{32} + k_2\alpha_2 Z_2)(e^{i2k_2h_2}-1)} \tag{8}$$

and

$$P(x,\omega) = (\lambda+2\mu)\frac{\partial w_1}{\partial x} = \rho_1\alpha_1^2\frac{dw_1}{dx} = F(\omega)\left(-e^{-ik_1x} + \mathrm{R}\cdot e^{ik_1(x-2h_1)}\right) \tag{9}$$

The pressure, $p(x, t)$, at a given point, x, can be calculated by inversion of $P(x,\omega)$ using FFT.

The properties of the three materials used in the calculations are given in Table 1. The pressure at the point, $x = 5\ mm$, marked by the symbol "⊕" is calculated for $\tau = 2\ \mu s$. The results are shown in Fig. 2.

Table 1. Material Properties used in Figs. 1 - 9.

Material	Density (*g/cc*)	P-Wave Speed (*mm/ms*)	S-Wave Speed *(mm/ms)*	Thickness (*mm*)
Water	1000	1500	0	15
Solid #1 [5]	2600	2800	1300	10
Solid #2 [5]	1180	2470	1080	∞
Aluminum	2700	6400	3200	∞
BIOM [5]	3900	1881	1038	5

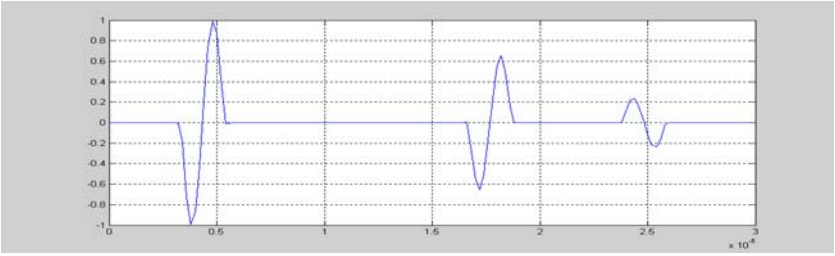

Fig. 2: Analytical solution for the pressure in the three-layered model at $x = 5.0\ mm$

2.3 FEM analysis using PZflex

The FEM calculations using PZflex are carried out in a model with finite dimensions: - 15 mm < y < 15 mm, 0 < x < 35 mm. The SYMM boundary is used on both sides of this strip, y = ± 15 mm, and the ABSR boundary condition is used at x = 35 mm to simulate the infinite dimension along the x direction. The pressure history at x = 5 mm in the fluid is shown in Fig. 3. Comparing the results obtained by theoretical method and FEM, we can see that the theoretical solution and numerical solution are almost identical. However, the small oscillation after the main pulse is caused by numerical noise generated by the FEM code.

As an example of the additional capabilities of the PZflex software, the full-field pressure at two different times, calculated from PZflex, are shown in Fig. 4. The interaction of the waves with the two interfaces can be easily identified.

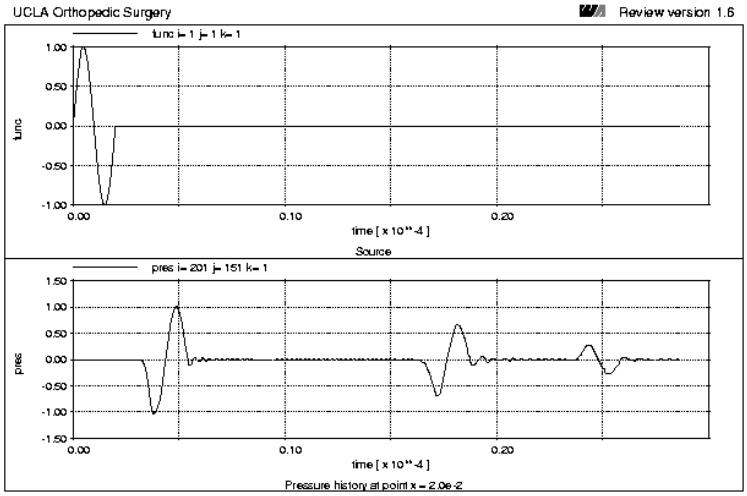

Fig. 3: FEM solution for the pressure in the three-layered model at $x = 5.0\ mm$

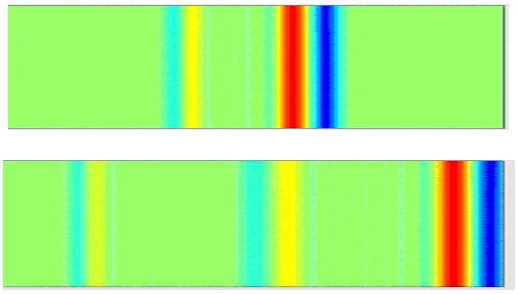

Fig. 4: Pressure distribution in the medium at $t = 13\ \mu s$ and $16\ \mu s$.

3. FOCUSED ULTRASOUND

It is well known that a focused lens can steer the beam into a point at higher energy than a uniform beam [8]. The mechanical effect of ultrasound in a material by a uniform load and a phase-delayed source that simulates focused ultrasound is calculated and compared by using PZFlex FEM analysis. In this section, the focused ultrasound is used and the mechanical effect is considered for three cases.

3.1 Focused wave in a two-layered medium

In the problem shown in Fig. 5, the pressure caused by a focused cylindrical lens is calculated. The materials used are water and aluminum; their mechanical properties are listed in Table 1. In Fig. 5, the part above the black line is water and the rest is aluminum. The angle of the lens is 60^o and its radius is *30 mm*.

The focal point of the lens is marked by the symbol "+" in the figure. The thickness of the water layer is 8 mm and the dimension of the FEM model is *60 mm × 60 mm*. All of the boundaries are ABSR boundaries. The applied pressure on the lens is the first half of the pulse given in equation (9).

The calculated wavefields are shown in Fig. 6. The "focal points" for the two cases: (a) water and aluminum, and (b) water only, are also shown. The input energy is the same but the pressure in the "focal point" is different for the two cases. The focal pressure in water is higher than that in aluminum; this is expected to be true for most solids including bones and other biological materials. Phase delay and other similar techniques can be used to increase the pressure in the solid.

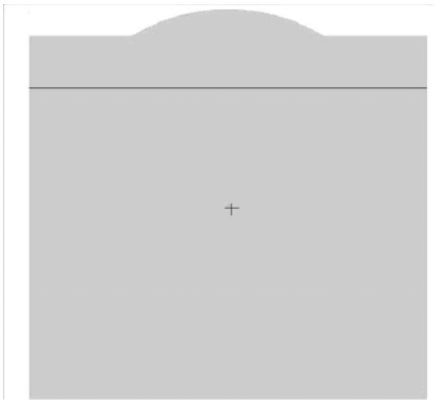

Fig.5: The geometry of the model

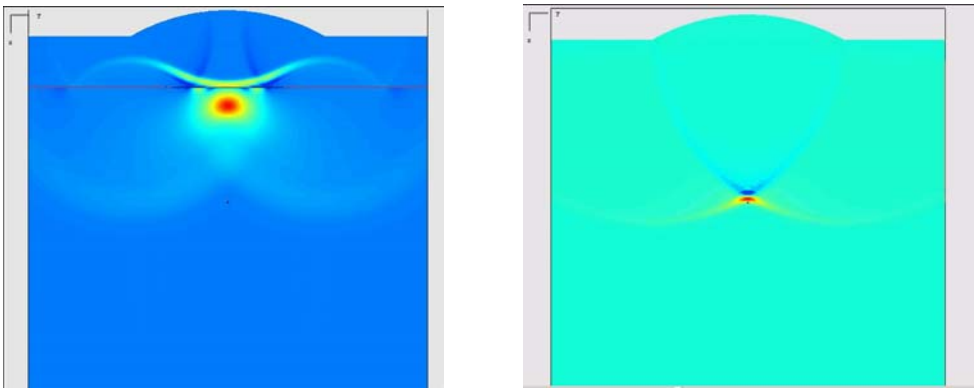

(a) In water-loaded aluminum (b) In water only

Fig. 6: The wavefields and "focal points"

It should be mentioned that the PZflex calculations presented in Fig. 6 produce significant "negative pressure" fields originating from the edges of the lens. Since the incident field in this case is a positive pressure pulse, the negative pressure field appears to be numerical noise associated with the FEM code.

3.3 Wave interaction with a biomaterial

In this section, we consider the interaction of the focused beam from the lens considered in the preceding section with a layer of a biomaterial (BIOM) with properties given in Table 1. These properties are close to those of human bone tissues. The simulation model is shown in Fig. 7(a), where the black arc is the lens, the middle layer is the bone, and the rest is water. The distance between the edges of the lens and the top surface of the layer is 5 mm. The result, presented in Fig. 7(b), shows that after the ultrasound passes through the layer, it is refocused at a point below the layer, as can be predicted on the basis of ray theory.

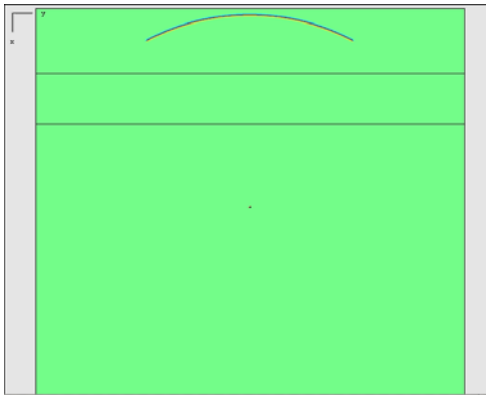

Fig. 7: (a) The geometry of the problem

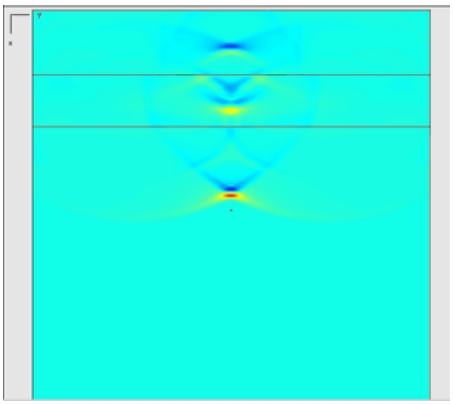

Fig. 7: (b) The refocused point

4. THE THERMAL FIELD

The thermal effects play the most significant role in many applications of therapeutic ultrasound. In this section, the quantitative features of the mechanical and thermal effects produced in a biomaterial insonified by a focused ultrasonic field (Fig. 8), is examined in this section. For simplicity, both materials are assumed to be semi-infinite. The biomaterial is assumed to be dissipative (viscoelastic) with loss factor, D, shown in Fig. 9 in units of db/m. The effects of dissipation on the acoustic wavefield can be incorporated in the calculations through the introduction of the non-dimensional specific attenuation factor, Q, related to D through the equation

$$Q \cong \frac{27.3f}{cD}$$

where f is the frequency in *MHz* and c is the phase velocity in *m/s*. The attenuation factor, Q, for the biomaterial is shown in Fig. 10. It is interesting to note that Q is approximately the same for dilatational and shear waves.

The temperature field produced in the material is governed by the modified heat equation,

$$\frac{\partial T}{\partial t} = \nabla \cdot (k \nabla T) + Q_u$$

where k is the thermal conductivity and Q_u is the dissipated (or absorbed) acoustic energy. Pzflex tracks the damping losses in the mechanical field and solves the discretized form of the heat equation using an implicit time integrator.

The thermal properties of the materials used in the calculations are given in Table 2. The lens is as the same as the one in last problem; its radius is 30 mm and the angle is 60^o. The dimensions of the finite element model are $60\ mm \times 60\ mm$. The incident ultrasound is a continuous pressure wave with frequency f, and amplitude 1MPa.

Table 2. Thermal properties of the materials used in the calculations

Material	Q *@1MHz*	Specific Heat *J/Kg·K*	Thermal Conductivity *W/mK·*
BIOM [5]	25	4200	0.058
Water	∞	4200	0.058

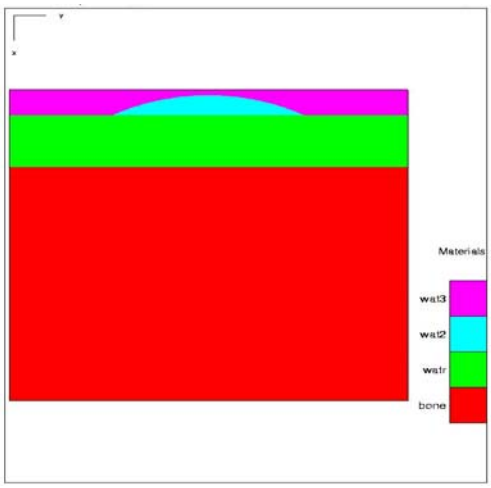

Fig. 8: The model of thermal problem

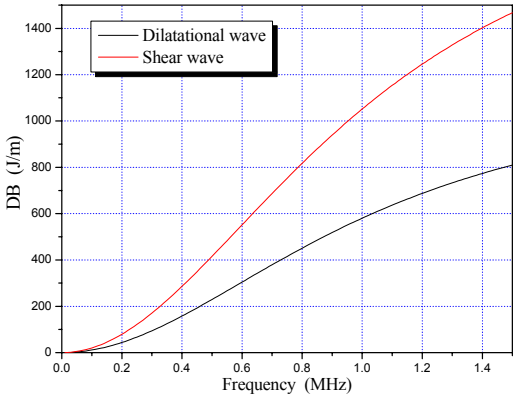

Fig. 9: Energy dissipation in the biomaterial as a function of frequency.

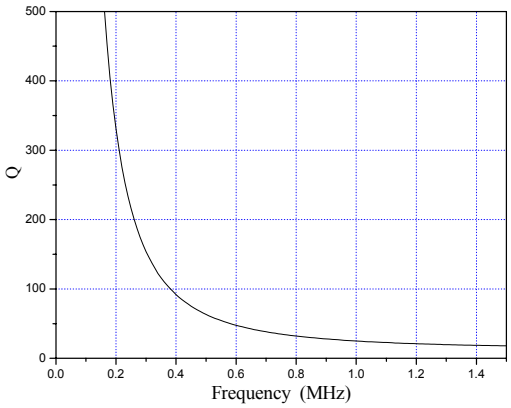

Fig. 10: Attenuation factor, *Q*, as a function of frequency in the biomaterial

4.2 Loss of energy and the temperature field

The calculated results are shown in Fig.11 for the case of frequency 500KHz. Fig.11 (a) is the steady state of the mechanical effect showing the pressure distribution for the continuous ultrasound wave. Fig.11 (b) shows the region of high energy loss - all of this area would be subjected to relatively high temperature.

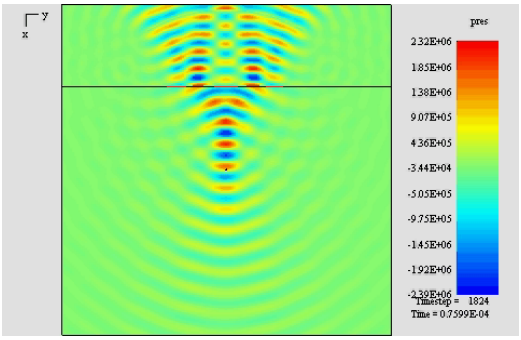

(a) Steady pressure field produced by a continuous wave.

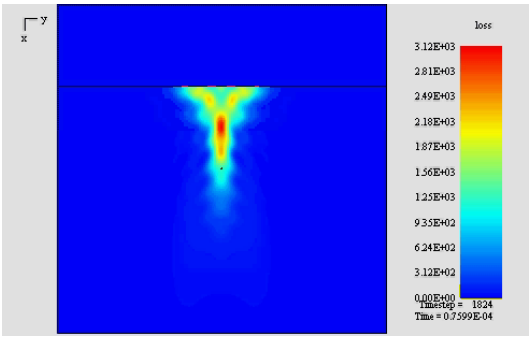

(b) Distribution of energy loss

Fig. 11: Calculated pressure field (a) and energy loss (*J*) in the biomaterial (b).

The temperature distributions caused by the focused ultrasound at three different frequencies, .5MHz, 1MHz, and 1.5 MHz are shown in Figs. 12. It can be seen that the temperature distributions in the three cases are qualitatively similar, but the peak temperatures in the focal region are strongly frequency dependent. This is shown in Fig. 13 where the calculated peak temperature produced in the focal region of the biomaterial is plotted as a function of the exciting frequency. It can be seen that the peak temperature in the focal region first increases then drops rapidly with frequency. At higher frequencies, the increase in temperature appears to occur primarily near the interface. The temperature increase in the focal region is plotted as a function of time in Fig. 13b. It can be seen that the increase is almost linear in time.

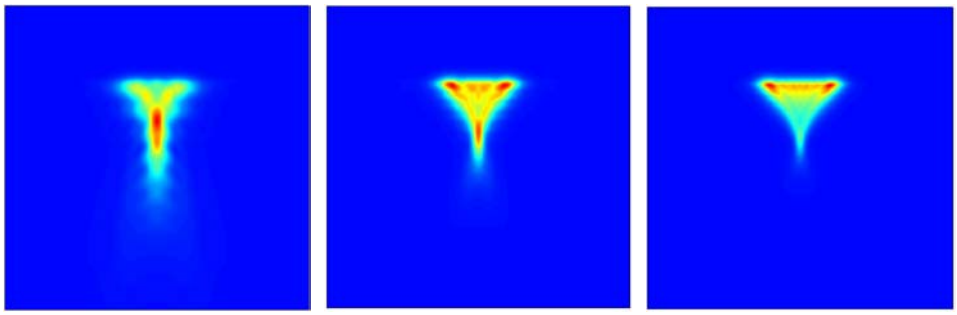

Fig.12: Temperature distributions in the biomaterial at 8 sec.
0.5 MHz (left panel), 1 MHz (middle panel) and 1.5MHz (right panel)

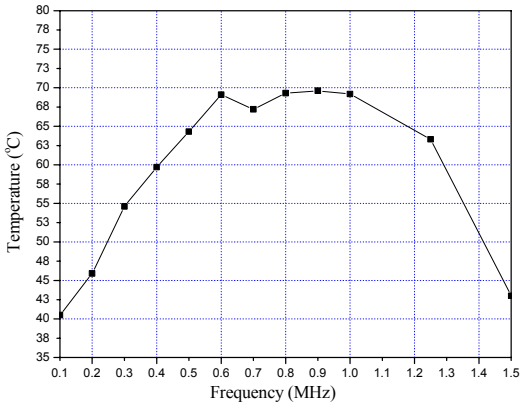

Fig. 13a: Peak temperature vs. frequency at 8 sec.

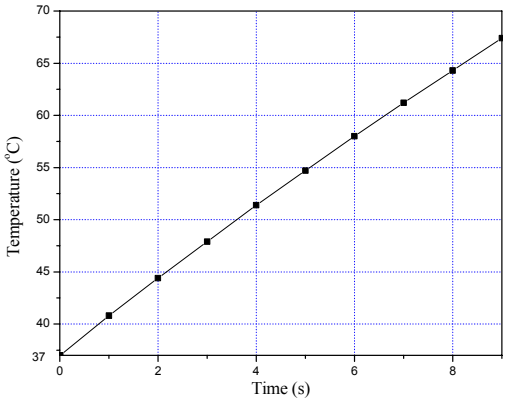

Fig. 13b: Peak temperature in the focal region as a function of time.

5. CONCLUSIONS AND FUTURE RESEARCH

Locating the focal region of therapeutic ultrasound in complex biological materials systems is an important issue that needs to be properly addressed before wider clinical applications are possible. Lack of adequate knowledge on the temperature distribution in the biomaterial can lead to thermal exposure to a larger area for longer period of time and use of higher intensity ultrasound than may be needed. The knowledge gathered not only can reduce the needed intensity of the input ultrasound, but also reduce possible damage to the surrounding tissues. The characteristics of the interaction between focused ultrasound and a simple model of the biological material have been determined in this paper. Several interesting features of the interaction including the shape and size of the focal region and the frequency as well as the spatial distribution of the temperature field in the material have been presented. Interaction with realistic models of biological materials systems and the effects of cavitation, bubble formation, nonlinear effects, etc. are under current investigation.

ACKNOWLEDGMENT

This research was supported by a grant from the Whitaker Foundation.

REFERENCES

1. P.D. Wall, W.J. Fry, R. Stephens, D. Tucker, and J.Y.Lettvin, "Changes produced in the central nervous system by ultrasound," *Sci*., **114**, pp. 686-687, 1951.
2. Sanghvi, N.T.; Fry, F.J.; Bihrle, R.; Foster, R.S.; Phillips, M.H.; Syrus, J.; Zaitsev, A.V.; Hennige, C.W. "Noninvasive surgery of prostate tissue by high-intensity focused ultrasound," *IEEE Transactions on Ultrasonics, Ferroelectrics and Frequency Control*, **43**, (No. 6), pp. 1099-110, Nov. 1996.
3. Seip, R.; VanBaren, P.; Cain, C.A.; Ebbini, E.S. **"**Noninvasive real-time multipoint temperature control for ultrasound phased array treatments," *IEEE Transactions on Ultrasonics, Ferroelectrics and Frequency Control*, **43**, (No.6), pp. 1063-73, Nov. 1996.
4. Bilgen, M.; Insana, M.F. **"**Effects of phase aberration on tissue heat generation and temperature elevation using therapeutic ultrasound,**"** *IEEE Transactions on Ultrasonics, Ferroelectrics and Frequency Control*, **43**, (No.6), pp. 999-1010, Nov. 1996.
5. PZflex Software, Version: 1-j.6. Weidlinger Associates. Inc, 2001.
6. C.I. Zanelli, C.W. Hennige, and N.T. Sanghvi, "Design and characterization of a 10 cm annular array transducer for high intensity focused ultrasound (HIFU) applications," *Proc. IEEE Ultrasonic symp.* 3, 1887-1890. **3**, pp. 1887-90, 1994.
7. Greg Wojcik, et al "Nonlinear pulse calculations and data in water and a tissue mimic," *Proc. IEEE Ultrasonic Symp.* **2**, pp. 1521-6, 1999.
8. G. Wojcik, J.Mould, F. Lizzi, etc. "Nonlinear modeling of therapeutic ultrasound," *Proc. IEEE Ultrasonic symp.* **2**, pp. 1617-22, 1995.
9. N. Abboud, et al, "Thermal generation, diffusion and dissipation in 1-3 piezocomposite sonar transducers: finite element analysis and experimental measurements," *Proc. IEEE Ultrasonic symp.* **2**, pp. 895-900, 1997.